

# Influence of CeO<sub>2</sub> on microstructure and microwave dielectric properties of Na<sub>1/2</sub>Sm<sub>1/2</sub>TiO<sub>3</sub> ceramics

Zi-xuan Fang<sup>1</sup> · Bin Tang<sup>1</sup> · Feng Si<sup>1</sup> · Shu-ren Zhang<sup>1</sup>

Received: 30 July 2015 / Accepted: 25 October 2015 / Published online: 28 October 2015  
© Springer Science+Business Media New York 2015

**Abstract** Crystal structures and microwave dielectric properties of wt% CeO<sub>2</sub>-added Na<sub>1/2</sub>Sm<sub>1/2</sub>TiO<sub>3</sub> (NST) ceramics were investigated systematically ( $x = 0.0, 0.3, 0.6, 0.9$  and  $1.2$ ). Samples with CeO<sub>2</sub> content  $\leq 1.2$  wt% were crystallized as single phase of orthorhombic perovskite structures. When Ce<sup>4+</sup> initially entered into the A-site of perovskite structure, uniform grain growth was observed and the dielectric constant increased, but then as Ce<sup>4+</sup> began to enter into the B-site of the perovskite structure, abnormal grains appeared and the  $\epsilon_r$  value reduced. The  $Q \times f$  value was firstly enhanced to its maxim value of 9640 GHz due to the improvement of density and elimination of pores as Ce<sup>4+</sup> content was in the range of 0.0–0.6 wt%, then sharply decreased. The temperature coefficient of resonant frequency ( $\tau_f$ ) slightly decreased from 199.7 to 185.1 ppm/°C. Typically, specimens sintered in air at 1425 °C for 2 h exhibited excellent microwave dielectric properties of  $\epsilon_r = 103.01$ ,  $Q \times f = 9640$  GHz and  $\tau_f = 192.8$  ppm/°C. The relationships between microwave properties and crystal structures were also discussed in this paper.

## 1 Introduction

In the recent several decades, microwave dielectric ceramics have revolutionized the wireless communication industry by reducing the size and cost of filter, oscillator

and antenna components in applications ranging from cellular phones to global positioning systems [1, 2]. In order to meet the grim and specific requirements of microwave applications, microwave dielectric materials must satisfy three major criteria: a high dielectric constant ( $\epsilon_r$ ) for miniaturization, a high quality factor ( $Q \times f$ ) or low dielectric loss ( $Q = 1/\tan\delta$ ) for better selectivity and near-zero temperature coefficient of resonant frequency ( $\tau_f$ ) for stable frequency stability. Microwave ceramics with high dielectric constant make it possible to noticeably miniaturize passive microwave components since the physical length of a dielectric resonator is proportional to  $1/\sqrt{\epsilon_r}$ . Hence, great efforts have been made to develop microwave ceramics with a high dielectric constant. And among them, the orthorhombic perovskite Na<sub>1/2</sub>Sm<sub>1/2</sub>TiO<sub>3</sub> ceramic was one of such promising materials with a high dielectric constant value of  $\epsilon_r = 80$  and extremely high quality factor of 13,000 GHz. However, its poor temperature coefficient of resonant frequency of 190 ppm/°C make it imperfect for the utilization as dielectric resonator [2]

As is generally known, Ceria (CeO<sub>2</sub>) has been universally employed to improve the comprehensive properties of dielectric ceramics, such as (PbCa)(FeNb)O<sub>3</sub>, Ba<sub>3</sub>Co<sub>0.7</sub>Zn<sub>0.3</sub>Nb<sub>2</sub>O<sub>9</sub> (Zr<sub>0.8</sub>,Sn<sub>0.2</sub>)TiO<sub>4</sub> and many other perovskite ceramic materials. For example, Zhou et al. [3] revealed that the dielectric constant was enhanced because of the improvement of densities and  $Q \times f$  values increased due to compensation effect on lattice vibration anharmonicity in Ce modified (PbCa)(FeNb)O<sub>3</sub> (PCFN)ceramics. For the Ce added Ba<sub>3</sub>Co<sub>0.7</sub>Zn<sub>0.3</sub>Nb<sub>2</sub>O<sub>9</sub> ceramics, Azough et al. [4] found that specimens with 0.4 wt% CeO<sub>2</sub> dopants showed maximum  $Q \times f$  value partly attributed to the high density, and  $\tau_f$  could be tuned to near zero value. What's more, Pamu et al. [5] reported that the quality factor were

✉ Bin Tang  
tangbin@uestc.edu.cn

<sup>1</sup> State Key Laboratory of Electronic Thin Films and Integrated Devices, University of Electronic Science and Technology of China, Chengdu 610054, China

significantly promoted to an extremely high value by adding 1.5 wt% CeO<sub>2</sub> to (Zr<sub>0.8</sub>,Sn<sub>0.2</sub>)TiO<sub>4</sub> (ZST)ceramics. But Ceria, as an effective aids for many ceramic system, hasn't researched in the high dielectric constant microwave ceramics such as Na<sub>1/2</sub>Sm<sub>1/2</sub>TiO<sub>3</sub> system.

In this paper, the effects of CeO<sub>2</sub> addition on the sintering behaviors, microstructures and microwave dielectric properties of Na<sub>1/2</sub>Sm<sub>1/2</sub>TiO<sub>3</sub> (NST) are systematically investigated with the variation of Ce content.

## 2 Experimental procedures

Samples of Na<sub>1/2</sub>Sm<sub>1/2</sub>TiO<sub>3</sub> microwave ceramics were synthesized by the conventional solid-state ceramic route. High-purity powders of Na<sub>2</sub>CO<sub>3</sub> (≥99.9 %, Mianyang Yuanda New Materials Co., Ltd, Mianyang, China), Sm<sub>2</sub>O<sub>3</sub> (99.9 %, Gansu Rare-earth New Materials Co., Ltd, Baiyin, China) and TiO<sub>2</sub> (99.9 %, Xiantao ZhongXing Electric Co., Ltd, Xiantao, China) were used as the starting materials. The raw oxide materials were weighted according to stoichiometry proportions of Na<sub>1/2</sub>Sm<sub>1/2</sub>TiO<sub>3</sub> with addition of 6 wt% Na<sub>2</sub>CO<sub>3</sub> powder, since sodium had a tendency to vaporize at high temperatures. The mixture of the starting materials was ball-milled in an alcohol medium for 10 h in a nylon jar using zirconia balls. The mixed slurry was dried, passed through a 100-mesh sieve and then calcined in air at 1100 °C for 3 h. Then the calcined NST powders were re-milled respectively with *x* wt% CeO<sub>2</sub> (*x* = 0.3, 0.6, 0.9 and 1.2) powders for 4 h. After drying, the powder was mixed with 5 wt% PVA binder, then dried and ground well. The obtained fine powder was axially pressed into cylindrical disks with the thickness of 6 mm and 15 mm in diameter under a pressure of 25 MPa. These pellets were sintered at different sintering temperatures from 1400 to 1500 °C for 2 h in air.

After sintering, the apparent densities of the samples were measured using the Archimedes method. The phase composition and crystal structure of the ceramics were examined by X-ray diffraction technique using CuKα radiation (Philips x'pert Pro MPD, Netherlands), and the lattice parameters and cell volume are obtained by computer software using unitcell. Raman spectra were collected by using Horiba Jobin–Yvon HR800 UV Raman spectrometer. The 632.6 nm line of He–Ne laser source were used as the exciting wavelength for these ceramic samples. Scanning electron microscopy (SEM) (SEM, FEI Inspect F, United Kingdom) was employed to study the surface morphology of the specimens. The dielectric characteristics at microwave frequencies were measured by the Hakki–Coleman dielectric resonator method in the TE<sub>011</sub> mode using a network analyzer (Agilent Technologies E5071C, the United States) and a temperature chamber (DELTA

9023, Delta Design, USA). The temperature coefficient of resonant frequency was determined from the difference between the resonant frequency obtained at 25 and 85 °C using the equation:  $\tau_f = (f_2 - f_1)/(f_1 \times (t_2 - t_1))$ , where  $f_1$  and  $f_2$  are the resonant frequencies at  $t_1 = 25$  °C and  $t_2 = 85$  °C, respectively.

## 3 Results and discussions

Figure 1 illustrates XRD patterns of NST ceramics doped with different amounts of CeO<sub>2</sub> sintered at their optimal sintering temperature for 2 h in air. According to the analysis of powder X-ray diffraction profiles [6, 7], all sintered samples were crystallized as orthorhombic perovskite structure and no secondary phases were detected throughout the whole scanning angles, implying that Ce<sup>4+</sup> ions had diffused into the crystal lattices of the mentioned samples and formed solid solutions. In our experimental work, weak super lattice reflections double the period of the primitive cell in an even even–odd and odd–odd–odd manner were also observed for whole specimens [6]. Furthermore, on closely examination, the  $2\theta$  diffraction angle in the XRD spectra firstly shifted to higher angle with *x* value varied from 0 to 0.6 wt% which suggested that the lattice parameter of the solid solution decreased because the relatively smaller ionic radii Ce<sup>4+</sup> of 12-coordinated (0.114 nm) entered the A-site of the perovskite structure occupied by (Na<sub>1/2</sub>Sm<sub>1/2</sub>)<sup>2+</sup> with the average size of 0.1315 nm [8]. Then as the *x* value further increased from 0.6 to 1.2 wt%, the  $2\theta$  began to move towards lower angle which meant the relatively larger ionic Ce<sup>4+</sup> of six-coordinated (0.087 nm) started to enter the B-site of the perovskite structure to substitute the Ti<sup>4+</sup> with the radii of

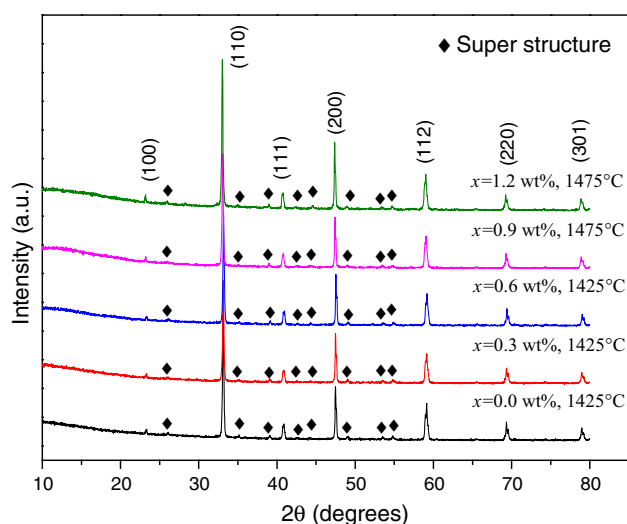


**Fig. 1** XRD patterns of NST ceramics doped with different amounts of CeO<sub>2</sub> sintered at their optimal sintering temperature for 2 h in air

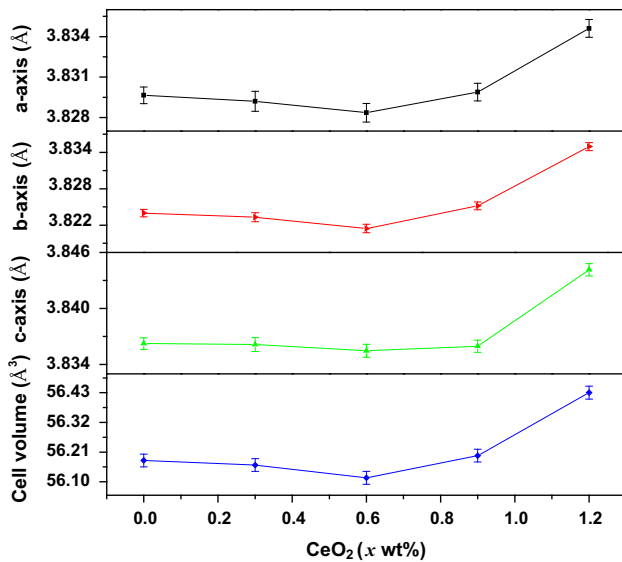


**Fig. 2** The lattice parameters and cell volumes of NST ceramics doped with different amounts of CeO<sub>2</sub> sintered at their optimal temperatures for 2 h in air

0.0605 nm and thus the lattice parameter increased. In order to comprehend the site occupancies and the effect of Ce<sup>4+</sup> on the A and B site, there was a necessity to have a refined calculation of lattice structure.

The lattice parameters and cell volume of NST ceramics doped with different amounts of CeO<sub>2</sub> sintered at their optimal temperatures for 2 h have been calculated, and are plotted in Fig. 2. It was apparent that with rising Ce content from 0.0 to 0.6 wt%, the a-axis, b-axis and c-axis slightly decreased, and thus their corresponding unit cell volumes also shrunk. This downward trend was mainly caused by the smaller ionic radii of Ce<sup>4+</sup> compared with that of (Na<sub>1/2</sub>Sm<sub>1/2</sub>)<sup>2+</sup> at A-site. But with  $x > 0.6$  wt%, lattice parameters presented a completely opposite trend, and all of them increased sharply, which was contributed to the larger ionic Ce<sup>4+</sup> incorporated into B sites at the oxygen octahedral. It was believable to understand our experimental results since a similar phenomenon was observed by Zhou et al. in (PbCa)(FeNb)O<sub>3</sub> ceramics. These calculation data strongly confirmed that the Ce<sup>4+</sup> could partially substitute for (Na<sub>1/2</sub>Sm<sub>1/2</sub>)<sup>2+</sup> at A-site within the Ce concentration of 0.6 wt% and replace the Ti<sup>4+</sup> at B-site when Ce content exceeded 0.6 wt%. At last, we could see varying trend of refined lattice parameters and cell volumes was in accordance with that of XRD patterns.

Raman spectrum was very useful for analysis of physical properties of the oxygen octahedral, its vibration manners and site substitutions, and Fig. 3 shows the Raman spectrum of NST ceramics doped with different amounts of CeO<sub>2</sub> sintered at their optimal sintering temperature. Actually, there exists changes in peaks position occurring at

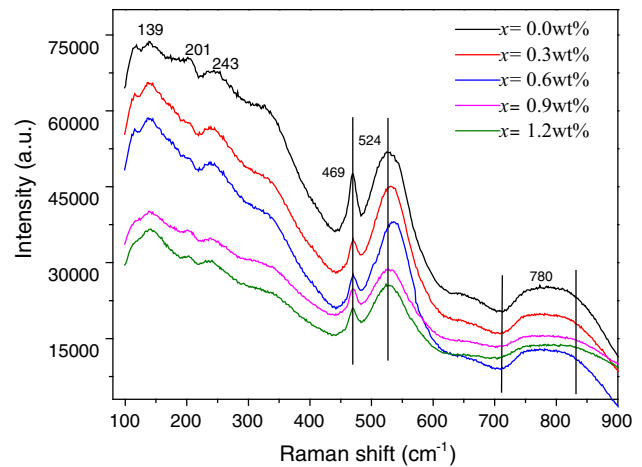
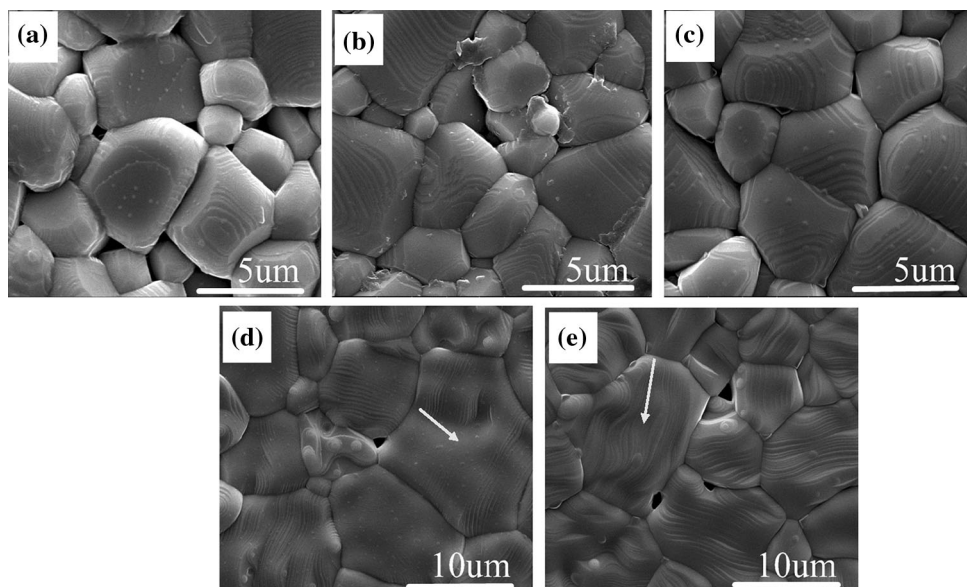


**Fig. 3** The Raman spectrum of NST ceramics doped with different amounts of CeO<sub>2</sub> sintered at their optimal sintering temperature for 2 h in air

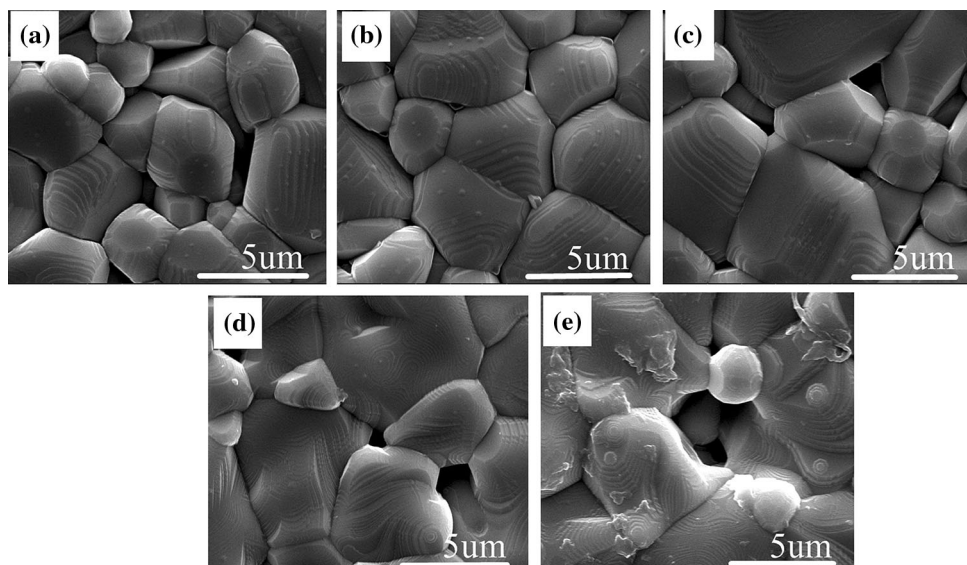
around  $\sim 524$  and  $780$  cm<sup>-1</sup> peak blueshift ( $\sim 524$  cm<sup>-1</sup>) is obviously observed at CeO<sub>2</sub> concentration from 0.0 to 0.6 wt%, while no clear peak shift is detected with  $0.9\% \leq x \leq 1.2$  wt%, which may be A-site cation related vibration contributed by oxygen atoms and an A-site cation [9]. Apparently, the peaks at around  $780$  cm<sup>-1</sup> broaden for  $0.9\% \leq x \leq 1.2$  wt% and shift slightly towards higher wavenumbers, which might be related to B-site substitution (vibration is confined in small regions with short-range correlations of atoms) [9, 10]. But there is no peak changes with  $0.0$  wt%  $\leq x \leq 0.6$  wt%. Hence, the results of Raman spectrum are corresponding to the analysis of XRD patterns.

For observing the effect of Ce concentrations on densification and grain size, the microstructure of samples is examined by Scanning Electron Microscopy (SEM), and Fig. 4 displays photographs of NST ceramics doped with different amounts of CeO<sub>2</sub> sintered for 2 h in air: (a)  $x = 0.0$  wt% 1425 °C, (b)  $x = 0.3$  wt% 1425 °C, (c)  $x = 0.6$  wt% 1425 °C, (d)  $x = 0.9$  wt% 1475 °C and (e)  $x = 1.2$  wt% 1475 °C. It was obvious that the addition of increasing amounts of Ce<sup>4+</sup> content severely affected the microstructure. Accompanied by the elimination of pores, the average grain size increased from 3 to 6  $\mu$ m with increase in wt% of CeO<sub>2</sub> up to 0.6 wt% and the homogeneous microstructure was observed with  $x = 0.6$  wt%. But subsequently, as directed by the white arrows in Fig. 4d, e, the abnormally grain growth occurred and inhomogeneous grains with average size of 9  $\mu$ m were presented when superfluous Ce content ( $x \geq 0.9$  wt%) was added to NST ceramics. Also, it could be seen that lots of pores appeared, and the grain edge and corner became blurred with  $x \geq 0.9$  wt%. The grain size increased apparently because of the incorporation of Ce<sup>4+</sup> ions into the grains and Ce addition enhanced the mass transport rate

**Fig. 4** SEM photographs of NST ceramics doped with amounts of CeO<sub>2</sub> sintered for 2 h in air: **a**  $x = 0.0$  wt% 1425 °C, **b**  $x = 0.3$  wt% 1425 °C, **c**  $x = 0.6$  wt% 1425 °C, **d**  $x = 0.9$  wt% 1475 °C and **e**  $x = 1.2$  wt% 1475 °C



**Fig. 5** SEM photographs of NST ceramics doped with 0.6 wt% CeO<sub>2</sub> sintered at different temperature: **a** 1400 °C, **b** 1425 °C, **c** 1450 °C, **d** 1475 °C, **e** 1500 °C for 2 h



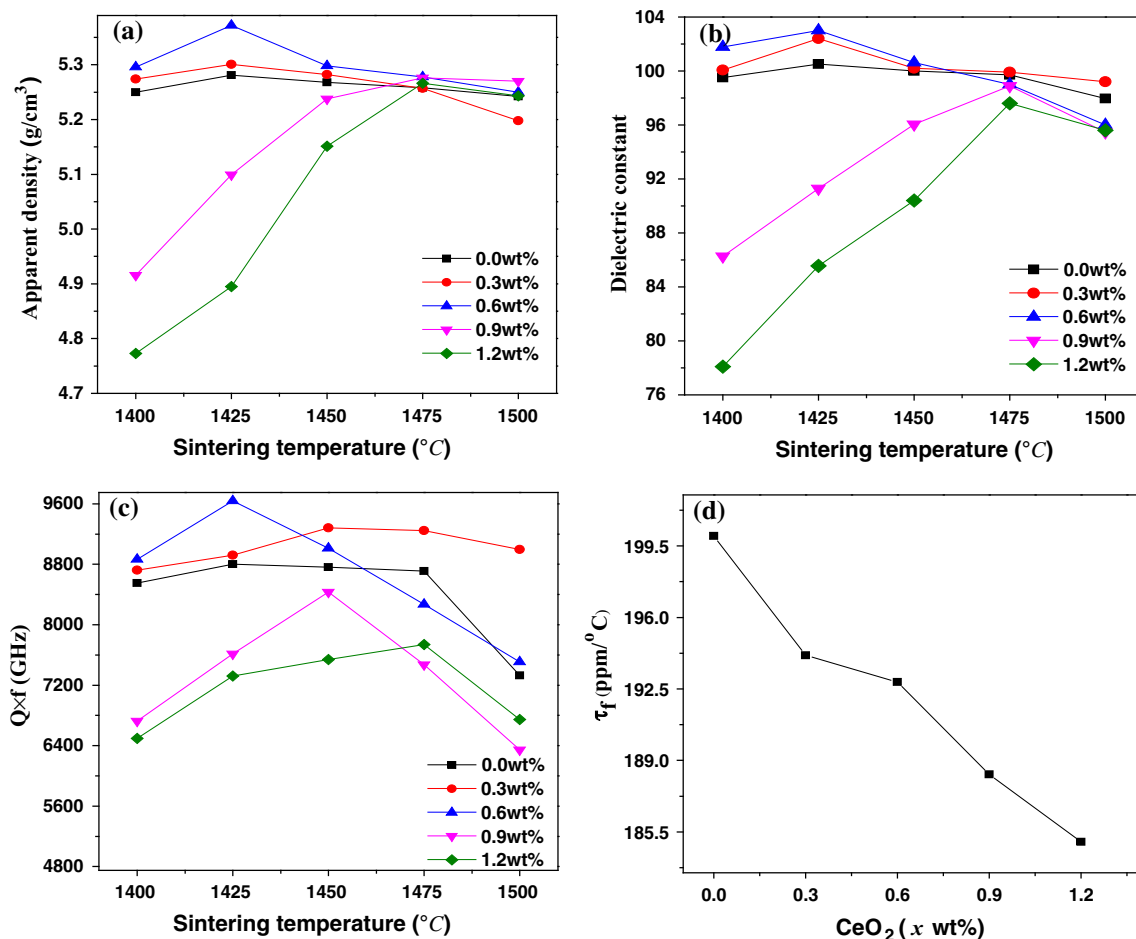
through a compensatory increase in oxygen vacancies. Sreemoolanadhan et al. [11] found a similar effect on the addition of Fe<sub>2</sub>O<sub>3</sub> to (Zr<sub>0.8</sub>, Sn<sub>0.2</sub>)TiO<sub>4</sub> ceramics.

Figure 5 presents SEM photographs of NST ceramics doped with 0.6 wt% CeO<sub>2</sub> sintered at different temperature: (a) 1400 °C, (b) 1425 °C, (c) 1450 °C, (d) 1475 °C and (e) 1500 °C for 2 h, respectively. It was clear that the porosity initially reduced, as sintering temperature increased from 1400 to 1425 °C, and meanwhile, the average grain size increased visibly with the sintering temperature rising. However, when sintered after 1425 °C, both the number and the size of pores increased with grain size growing over 6 μm. When sintered after 1475 °C, the apparent changes were observed to be that the larger hole

appeared, as shown in Fig. 5e. This is because during the over-sintering process, grain size grew rapidly to form coarse and big grains, at the same time, more and larger pores appeared [12]. Thereafter, the density of the pellet was reduced.

Figure 6 presents the apparent density and microwave dielectric properties of NST ceramics doped with different amounts of CeO<sub>2</sub> sintered at 1400–1500 °C for 2 h in air. As demonstrated in Fig. 6a, the apparent density of Ce-added NST ceramics first acutely went up owing to the improvement of densification as the sintering temperature increased, and thereafter the apparent density declined slightly because of the over-sintering process, as confirmed by SEM in Fig. 6d, e. Simultaneously, the apparent density





**Fig. 6** **a** Apparent density, **b** dielectric constant, **c** quality factor and **d** temperature coefficient of resonant frequency of NST ceramics doped with different amounts of CeO<sub>2</sub> sintered at 1400–1500 °C for 2 h in air

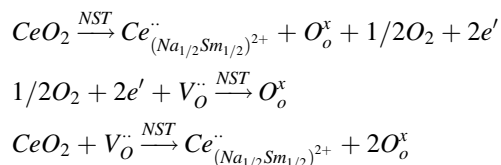
also showed a strongly dependent on CeO<sub>2</sub> content. The optimal apparent density of every fixed CeO<sub>2</sub> content initially displayed an improved trend and increased with *x* from 0.0 to 0.6 wt% which primarily resulted from the elimination of pores pinned at the boundary of matrix grains with growing average grain size [13]. However, when the Ce concentrations exceeded 0.6 wt%, optimal apparent density declined and it was mainly due to the abnormal grain growth [14], as shown in Fig. 4c–e. Abnormally growing grains, implying high levels of pores, should result in the decrease of apparent density.

Figure 6b shows variation of the dielectric constant versus the different sintering temperature. It was apparent that its varying tendency of every fixed Ce composition was almost in agreement with the change of the apparent density in their own temperature range. It is because both of the apparent density and dielectric constant are influenced much by many of the same reasons such as the densification process and pores. On the other hand, the dependence of dielectric constant on the Ce concentration could be divided into two stages. The first stage for the slight increase of the

dielectric values from 100.51 at *x* = 0.0 wt% to 103.01 at *x* = 0.6 wt% and the second stage for the continuous decline to 97.6 with *x* = 1.2 wt%. It is generally considered that dielectric constant is affected by many factors, such as density, polarizability, and unit cell volume [15, 16]. The dielectric constant was increased slightly in the range of 0.0 wt% < *x* ≤ 0.6 wt%, which should be mainly caused by the improvement of density. From another point of view, the dielectric constant improved with because of the larger ionic polarizability of Ce<sup>4+</sup> ( $\alpha = 3.94 \text{ \AA}$ ) compared with that of (Na<sub>1/2</sub>Sm<sub>1/2</sub>)<sup>2+</sup> ( $\alpha = 3.27 \text{ \AA}$ ) [17] at A-site. When it came to the second stage, the dielectric constant sharply dropped from 103.01 to 97.6 when the Ce concentration was raised from 0.9 to 1.2 wt%. Firstly, the decrease of  $\epsilon_r$  by substitution of Ce occurred because a slightly large Ce<sup>4+</sup> ion (0.807 Å) was incorporated to a Ti<sup>4+</sup> site with smaller ionic radii (0.605 Å), therefore it became more difficult to be displaced by the electrical field force. Secondly, the expansion of the cell volumes caused by Ce<sup>4+</sup> substitution at B-site may also be responsible for severe degradation of dielectric constant (degradation of

polarizability). What's more, in the superfluous Ce adding range ( $x \geq 0.9$  wt%), the decrease of density should primarily lead to the degradation of dielectric constant since the dielectric constant was strongly influenced by densities and pores ( $\epsilon_r = 1$ ).

For the quality factor as described in Fig. 6c, it was clearly seen that the  $Q \times f$  value varied dramatically as the variation of Ce content and sintering temperature.  $Q \times f$  value for the dependence on Ce concentrations firstly increased, then reached a saturated value of 9640 GHz at the point of  $x = 0.6$  wt%, and finally decreased with further increasing the Ce content. As reported in many literatures, the  $Q \times f$  values can be contributed to many extrinsic factors such as density, microstructures, grain size, and oxygen vacancies [18, 19]. And the oxygen vacancies contributed greatly to the dielectric loss. But in this case, the oxygen vacancies may be reduced by  $\text{Ce}^{4+}$  entering into the A-sites:



Hence, the elimination of oxygen vacancies may be partly responsible for the improvement of quality factor with  $0.0 \text{ wt}\% < x \leq 0.6 \text{ wt}\%$ . Moreover,  $Q \times f$  value also followed a similar trend as that of density versus wt% of  $\text{CeO}_2$ . The increase in  $Q \times f$  value with 0.6 wt% addition of  $\text{CeO}_2$  was attributed to their higher densities, uniform grain growth and higher average grain size. However, declination of densities (lots of pores), abnormally grain growth and quite inhomogeneous microstructures were observed with  $x \geq 0.9$  wt%. And large grains in dielectric ceramics are usually associated with more defects, such as dislocations, planar defects, and even the dislocation networks, which would lead to the decrease of the  $Q \times f$  values to some extent. Therefore, the decrease in the  $Q \times f$  values should be partially due to the grain size, microstructures and pores.

Figure 5d exhibits temperature coefficient of resonant frequency ( $\tau_f$ ) of NST ceramics sintered at their optimal temperature as the function of different amounts of  $\text{CeO}_2$ . The changing  $\tau_f$  is generally considered to be correlated with composition [20], secondary phase [21] and B-site bond valence [22]. Apparently, the  $\tau_f$  value did not change much and decreased slightly from 199.7 to 185.1 ppm/°C. Since the addition of  $\text{CeO}_2$  did not affect the compositions and cause any noticeable secondary phase, the improvement of temperature coefficient of resonant frequency may be related to the changing B-site bond valence. As previously reported, the increasing amounts of  $\text{CeO}_2$  led to a decrease in temperature coefficient of resonant frequency

in PCFN ceramics which was mainly contributed to the varying value of B-site bond valence [3]. A similar effect that  $\text{CeO}_2$  additions didn't intensively change the  $\tau_f$  value was observed in ZST systems [5]. Hence, it was believable to comprehend our experimental results.

In summary, when added with 0.6 wt%  $\text{CeO}_2$ , the NST ceramics sintered at 1425 °C for 2 h possessed excellent comprehensive properties of  $\epsilon_r = 103.01$ ,  $Q \times f = 9640$  GHz and  $\tau_f = 192.8$  ppm/°C. In addition to the greater densities and more homogeneous microstructure, NST ceramics prepared by Ce addition showed microwave dielectric properties of NST ceramics were superior to that of the pure  $\text{Na}_{1/2}\text{Sm}_{1/2}\text{TiO}_3$  ceramics ( $\epsilon_r = 79$ ,  $Q \times f = 8139$  GHz and  $\tau_f = 190$  ppm/°C) [23].

## 4 Conclusions

The influences of  $\text{CeO}_2$  additions on crystal lattice, microstructures, sintering behaviors and microwave dielectric properties of  $\text{Na}_{1/2}\text{Sm}_{1/2}\text{TiO}_3$  ceramics were systematically investigated in this study. All sintered samples were crystallized as orthorhombic perovskite structure and no secondary phases were detected. In the minor adding range of 0.0–0.6 wt%,  $\text{Ce}^{4+}$  firstly entered into A-site of perovskite structure. Meanwhile the average grain size increased, microstructure became uniform and the dielectric constant increased from 100.51 to 103.01. But with superfluous Ce content ( $x \geq 0.9$  wt%), then  $\text{Ce}^{4+}$  began to entered into B-site. Abnormal grain growth and inhomogeneous microstructure were observed as well as the degradation of dielectric constant to 97.6. The quality factor initially improve from 8803 to 9640 GHz in the range of 0.0–0.6 wt%, then sharply decreased 7740 GHz. It was found that a certain amount of  $\text{Ce}^{4+}$  entering into A-site of the perovskite could compensate the extrinsic loss caused by oxygen vacancies and result in a uniform grain growth, but a superfluous amount of  $\text{Ce}^{4+}$  diffusing into B-site of perovskite would lead abnormally grain growth and lots of pores. The  $\tau_f$  value did not change much and decreased slightly from 199.7 to 185.1 ppm/°C. Typically, the  $\text{Na}_{1/2}\text{Sm}_{1/2}\text{TiO}_3$  ceramic sintered in air at 1425 °C for 2 h exhibited good microwave dielectric properties of  $\epsilon_r = 103.01$ ,  $Q \times f = 9640$  GHz and  $\tau_f = 192.8$  ppm/°C.

**Acknowledgments** This work is supported by National Natural Science Funds of China (Grant No. 51402039).

## References

1. B. Tang, Z.-X. Fang, H. Li, L. Liu, S.-R. Zhang, Microwave dielectric properties of  $\text{H}_3\text{BO}_3$ -doped  $\text{Ca}_{0.61}\text{La}_{0.39}\text{Al}_{0.39}\text{Ti}_{0.61}\text{O}_3$  ceramics. *J. Mater. Sci. Mater. Electron.* **26**, 300–306 (2015)

2. M.T. Sebastian, *Dielectric Materials for Wireless Communication* (Elsevier, Amsterdam, 2010)
3. Z. Dong-xiang, H. Ming-zhe, J. Sheng-lin, H. Jing, Microwave properties of CeO<sub>2</sub>-modified (PbCa)(FeNb)O<sub>3</sub> dielectric ceramics. *Mater. Lett.* **58**, 2684–2687 (2004)
4. F. Azough, C. Leach, R. Freer, Effect of CeO<sub>2</sub> on the sintering behaviour, cation order and properties of Ba<sub>3</sub>Co<sub>0.7</sub>Zn<sub>0.3</sub>Nb<sub>2</sub>O<sub>9</sub> ceramics. *J. Eur. Ceram. Soc.* **26**, 1883–1887 (2006)
5. D. Pamu, G.L.N. Rao, K.V. Saravanan, K.C.J. Raju, Effect of CeO<sub>2</sub> and Nd<sub>2</sub>O<sub>3</sub> on the microstructure and microwave dielectric properties of (Zr<sub>0.8</sub>, Sn<sub>0.2</sub>)TiO<sub>4</sub> ceramics. *Integr. Ferroelectr.* **117**, 118–128 (2010)
6. H. Sun, T. Pai, Y.-J. Nakamura, Y. Shan, Inaguma and M. Itoh, High temperature quantum paraelectricity in perovskite-type titanates Ln<sub>1/2</sub>Na<sub>1/2</sub>TiO<sub>3</sub> (Ln = La, Pr, Nd, Sm, Eu, Gd and Tb). *Ferroelectrics* **200**, 93–107 (1997)
7. S.K. Barik, R.N.P. Choudhary, P.K. Mahapatra, Impedance spectroscopy study of Na<sub>1/2</sub>Sm<sub>1/2</sub>TiO<sub>3</sub> ceramic. *Appl. Phys. A* **88**, 217–222 (2007)
8. R.T. Shannon, C.T. Prewitt, Effective ionic radii in oxides and fluorides. *Acta Crystallogr. Sect. B* **25**, 925–946 (1969)
9. S. Ye, C.-H. Wang, X.-P. Jing, Photoluminescence and Raman spectra of double-perovskite Sr<sub>2</sub>Ca (Mo/W) O<sub>6</sub> with A- and B-site substitutions of Eu<sup>3+</sup>. *J. Electrochem. Soc.* **155**, J148–J151 (2008)
10. D. Scarano, A. Zecchina, S. Bordiga, F. Geobaldo, G. Spoto, G. Petrini, G. Leofanti, M. Padovan, G. Tozzola, Fourier-transform infrared and Raman spectra of pure and Al-, B-, Ti- and Fe-substituted silicalites: stretching-mode region. *J. Chem. Soc. Faraday Trans.* **89**, 4123–4130 (1993)
11. H. Sreemoolanadhan, R. Ratheesh, M. Sebastian, N. Rodrigues, J. Philip, The synthesis, characterization and properties of Hf-substituted (dielectric ceramics). *J. Phys. D Appl. Phys.* **30**, 1809 (1997)
12. X. Sha, Z. Lü, X. Huang, J. Miao, Z. Liu, X. Xin, Y. Zhang, W. Su, Influence of the sintering temperature on electrical property of the Ce<sub>0.8</sub>Sm<sub>0.1</sub>Y<sub>0.1</sub>O<sub>1.9</sub> electrolyte. *J. Alloys Compd.* **433**, 274–278 (2007)
13. H. Chen, B. Tang, A. Gao, S. Duan, H. Yang, Y. Li, H. Li, S. Zhang, Aluminum substitution for titanium in Ba<sub>3.75</sub>Nd<sub>0.5</sub>Ti<sub>18</sub>O<sub>54</sub> microwave dielectric ceramics. *J. Mater. Sci. Mater. Electron.* **26**, 405–410 (2015)
14. S.H. Yoon, D.-W. Kim, S.-Y. Cho, K.S. Hong, Investigation of the relations between structure and microwave dielectric properties of divalent metal tungstate compounds. *J. Eur. Ceram. Soc.* **26**, 2051–2054 (2006)
15. N.I. Santha, M.T. Sebastian, P. Mohanan, N.M. Alford, K. Sarma, R.C. Pullar, S. Kamba, A. Pashkin, P. Samukhina, J. Petzelt, Effect of doping on the dielectric properties of cerium oxide in the microwave and far-infrared frequency range. *J. Am. Ceram. Soc.* **87**, 1233–1237 (2004)
16. L. Fang, Y. Tang, D. Chu, H. Zhou, H. Zhang, X. Chen, Q. Liu, Effect of B<sub>2</sub>O<sub>3</sub> addition on the microstructure and microwave dielectric properties of Li<sub>2</sub>CoTi<sub>3</sub>O<sub>8</sub> ceramics. *J. Mater. Sci. Mater. Electron.* **23**, 478–483 (2012)
17. R.T. Shannon, Revised effective ionic radii and systematic studies of interatomic distances in halides and chalcogenides. *Acta Crystallogr. Sect. A* **32**, 751–767 (1976)
18. S. Yu, S. Zhang, B. Tang, X. Zhou, Y. Fang, Microwave dielectric properties of BaO–2(1 – x)ZnO–xNd<sub>2</sub>O<sub>3</sub>–4TiO<sub>2</sub> (x–1.0) ceramics. *Ceram. Int.* **38**, 613–618 (2012)
19. C.-F. Tseng, T.-C. Wei, S.-C. Lu, Influence of A-site Ba substitution on microwave dielectric properties of (Ba<sub>x</sub>Mg<sub>1–x</sub>)(A<sub>0.05</sub>–Ti<sub>0.95</sub>)O<sub>3</sub> (A=Zr, Sn) ceramics. *Ceram. Int.* **40**, 7081–7085 (2014)
20. Y. Li, H. Li, J. Li, B. Tang, S. Zhang, H. Chen, Y. Wei, Effect of TiO<sub>2</sub> ratio on the phase and microwave dielectric properties of Li<sub>2</sub>ZnTi<sub>3+x</sub>O<sub>8+2x</sub> ceramics. *J. Electron. Mater.* **43**, 1107–1111 (2014)
21. G.-H. Chen, C.-L. Yuan, C.-R. Zhou, Y. Yang, Low-firing high permittivity Ca<sub>0.6</sub>Sm<sub>0.8/3</sub>TiO<sub>3</sub>–(Li<sub>0.5</sub>Nd<sub>0.5</sub>)TiO<sub>3</sub> ceramics with BaCu(B<sub>2</sub>O<sub>5</sub>) addition. *Ceram. Int.* **39**, 9763–9766 (2013)
22. H.S. Park, K.H. Yoon, E.S. Kim, Relationship between the bond valence and the temperature coefficient of the resonant frequency in the complex perovskite (Pb<sub>1–x</sub>Ca<sub>x</sub>)[Fe<sub>0.5</sub>(Nb<sub>1–y</sub>Ta<sub>y</sub>)<sub>0.5</sub>]O<sub>3</sub>. *J. Am. Ceram. Soc.* **84**, 99–103 (2001)
23. H. Takahashi, Y. Baba, K. Ezaki, Y. Okamoto, K. Shibata, K. Kuroki, S. Nakano, Dielectric characteristics of (A<sub>1/2</sub><sup>1+</sup>·A<sub>1/2</sub><sup>3+</sup>)TiO<sub>3</sub> ceramics at microwave frequencies. *Jpn. J. App. Phys.* **30**, 2339 (1991)